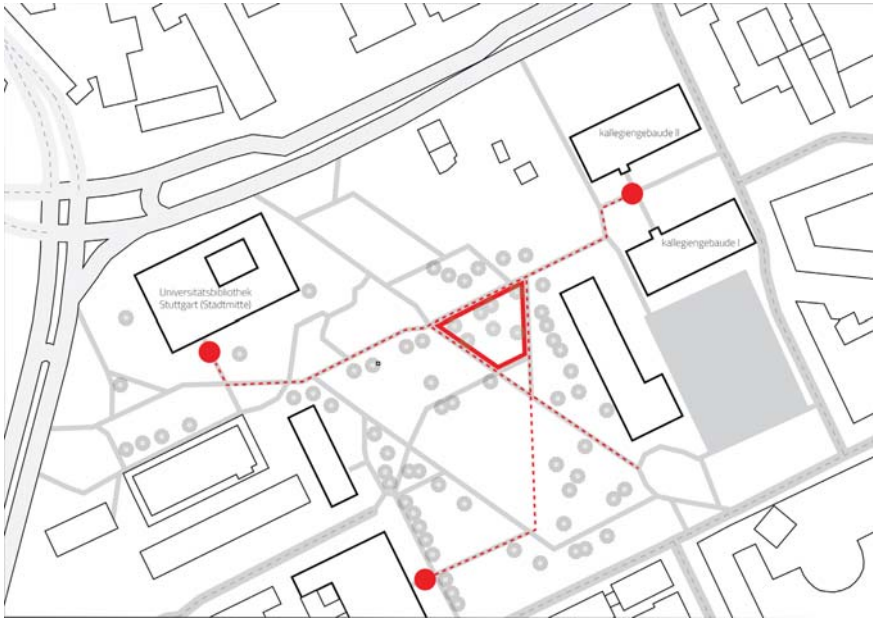


**FIGURE 1_1:** pedestrian flow around site (*Source: Jingcheng Chen, Olga Kalina (2015)*)

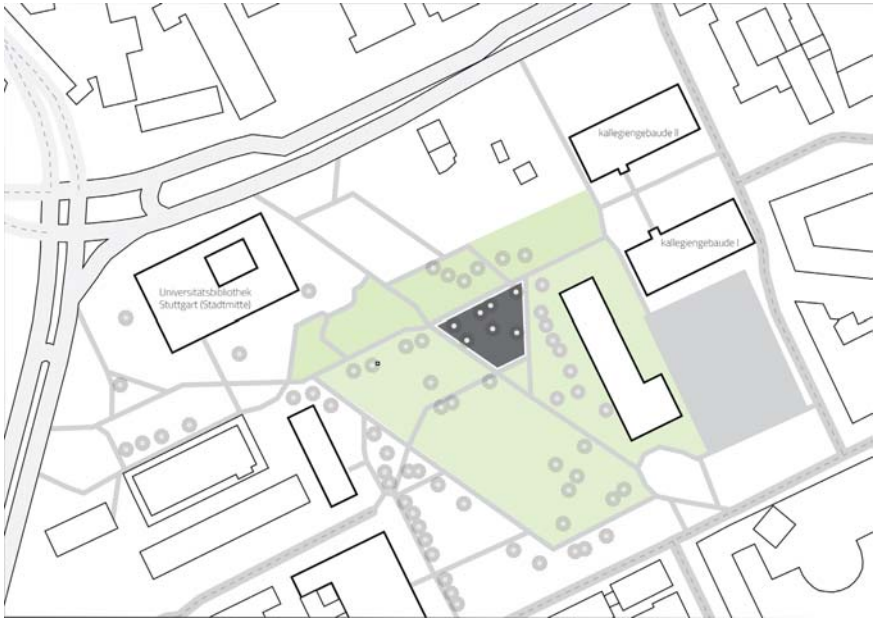


**FIGURE 1_2:** greening around site (*Source: Jingcheng Chen, Olga Kalina (2015)*)

## Site Analysis

The site of our pavilion is located in the very centre of the campus of Stuttgart University, where three main pedestrian flow would occur: one from the library and the cafeteria, one from two main teaching buildings and one from another school.

These three pedestrian streams take full usage of the roads around the site, which makes the triangular site quite symmetrical and central. This inspired us that a symmetrical and also triangular form of pavilion would be fitting the site condition.(Figure 1_1)

Another strong feature is that our site is totally surrounded by greenings and trees, where people want to appreciate but have no facilities such as seats and canopies. (Figure 1_3)

So, it would be good that our pavilion can provide a place to appreciate the whole landscape with seats. In this case, our pavilion should also be very transparent in order not to block the views.(Figure 1_2)


**FIGURE 1_3:** site aerial view (*Source: Google Maps (2015)*)

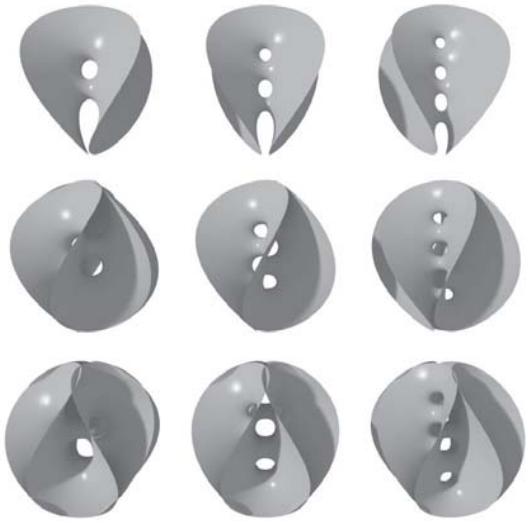

**FIGURE 2_1:** Different configurations of Chen-Gackstatter Surface. (*Source: http://mathworld.wolfram.com/Chen-GackstatterSurfaces.html*)

*The Chen–Gackstatter surface family is a family of minimal surfaces that generalize the Enneper surface by adding handles, giving it nonzero topological genus. It was the first completely immersed minimal torus of finite total curvature, discovered in 1981. It is an isolated surface with one Enneper end. It is possible to increase the dihedral symmetry.*

*---- Thayer, Edward C. (1995)*

## Form Inspiration

In the first place we were attracted by mathematical definition and configuration of minimal surface.

In mathematics, a minimal surface is a surface that locally minimizes its area. This is equivalent to having a mean curvature of zero. 'Minimal surfaces' are the smallest surfaces and the minimal energy form within defined boundaries, and the surface tension is equal and uniform at any point.(Wikipedia)

According to the definition of minimal surface, we can conclude that from structural point of view, there are several benefits of using the form of minimal surface:

- Structural efficiency
- Efficient material distribution
- Overall area minimization

Therefore, we looked for various kinds of minimal surfaces and found Chen-Gackstatter Surface. Given different parameters configuration, we can deduce to a differentiated form of minimal surface, where we can choose the shape with three sides and at the same time centre-symmetrical.

## Structural Concept

In the sense that in attempt to achieve the form of minimal surface, bending-active material would be an ideal solution for the frame of the surface, which can be fabricated from initially planar geometry, making the whole fabrication process simpler and more efficient.

In addition, we discovered a lot resemblance between membrane structure and minimal surface (initially we attempted to use membrane as part of our structure), which makes it easier to achieve the final geometry that we needed.

**FIGURE 2_2:** usage of bending-active structure. (*Source: ICD/ITKE Research Pavilion 2010*)

**FIGURE 2_3:** bending-active material in pole vault. (*Source: Block Research Group*)

*"Bending-active structures are structural systems that include curved beam or shell elements which base their geometry on the elastic deformation from an initially straight or planar configuration."*

*---- Julian Lienhard et al. (2011)*

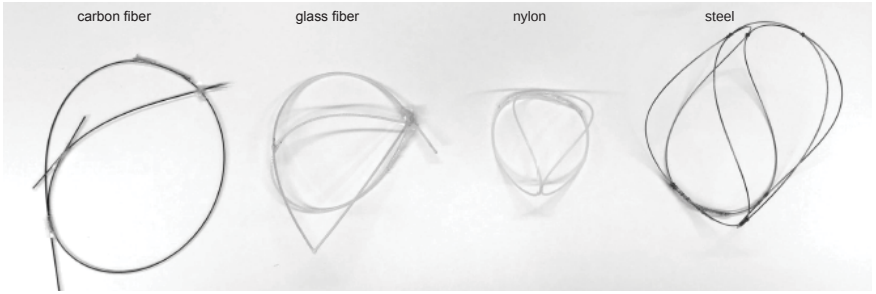


**FIGURE 3_1:** different material tests for frame. (*Source: Jingcheng Chen, Olga Kalina*)

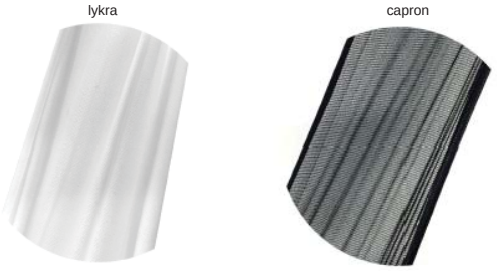


**FIGURE 3_2:** different material tests for membrane. (*Source: Jingcheng Chen, Olga Kalina*)

## Material Test

In order to better understand the properties of the material that may be in use for our structures, we first selected different material for the physical test.

As mentioned before, in the beginning we attempted to use a membrane and bending-active frame as our structural combination, aiming to find a proper form that fulfils the minimal surface concept and as well structurally practical with certain material. For our first experiments with the materials we choose several examples for each part of the structure.

For the bending-active frame we tested carbon fiber, glass fiber, nylon and steel pipes. From a variety of experiments we find steel rods show best performance in bending for small scale whereas the glass and carbon fiber rods were fragile and not so flexible when bending extremely into a small radius. The nylon pipes were good at the beginning but after some bending actions the pipes were bent in perpetuity.

From the huge number of different elastic fabrics, we came to the agreement that the textile itself has to be structurally equally elastic in two dimensions, also, soft and thin enough to work on a small scale. For that reason the Capron was chosen.

We made a few physical models and found that it is quite difficult to deal with membrane and bending-active rod since we have to apply pre-tensioned force to the membrane which comes to all directions on the 2D surface and leads to a complex simulation model as well as fabrication process.

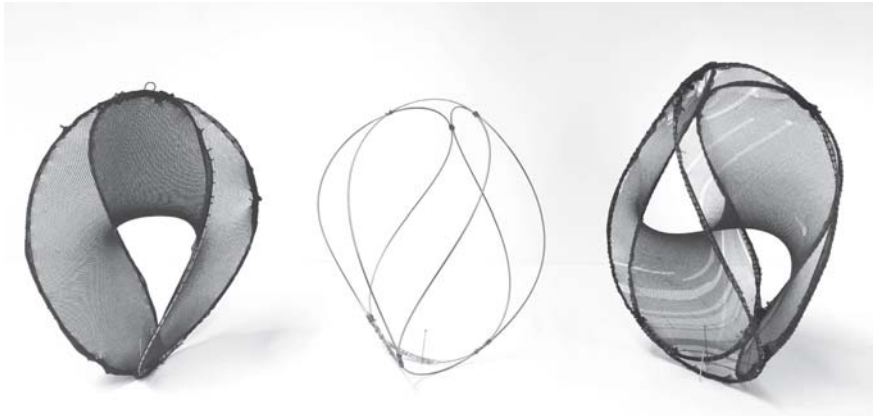

**FIGURE 3_3:** experimental physical models. (*Source: Jingcheng Chen, Olga Kalina*)

**FIGURE 3_4:** experimental physical models. (*Source: Jingcheng Chen, Olga Kalina*)

## Form Finding Exploration

According to the physical form finding tests of the Chen-Gackstatter shape we moved to its computational simulations, trying to find a practical and at the same time aesthetically elegant form.

The goal was to understand how to achieve a 3D complex structure from the planar basis. The circular shape is squeezed in the first place inwards. Then applying inner and outer trigger forces vertically, the shape will start to deform into a force equilibrium and change into stable geometry.

As you can see from the right side(Figure 3_5), we simulated the an outer circular frame as bending-active material. And all the inner grid we simulated as a membrane. We apply a pre-tensioned force to the membrane to let it try to shrink. And at the same time a trigger force is added vertically, which will be released after the equilibrated shape is formed.

In a geometrical boundary we found out that theoretically there is almost no limit to the number of sides. It starts from two sides, and the more the number of the side is, the flatter the centre of the form will be. According to our initial architectural desires and a form with certain undulation, we chose the triangular shape for our further explorations and studies.

two-sides form finding

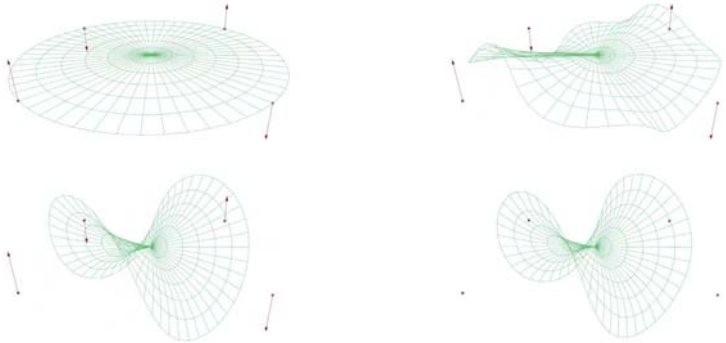

three-sides form finding

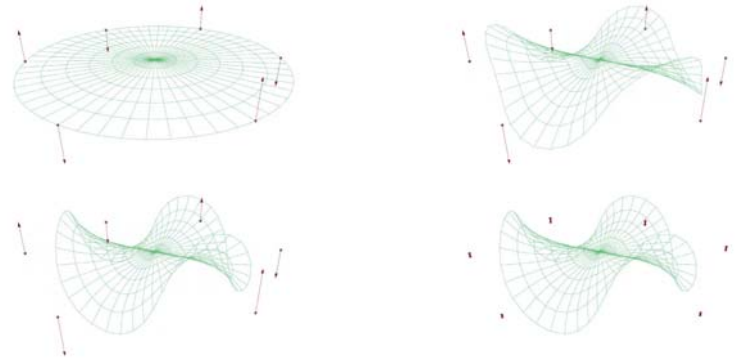

six-sides form finding

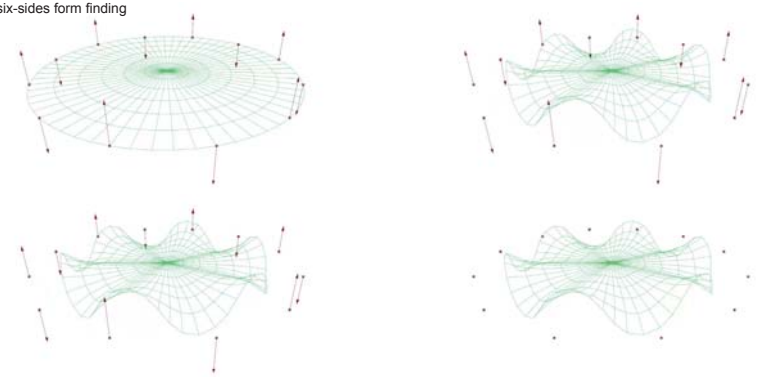

**FIGURE 3_5:** computational form finding process. (*Source: Jingcheng Chen, Olga Kalina*)

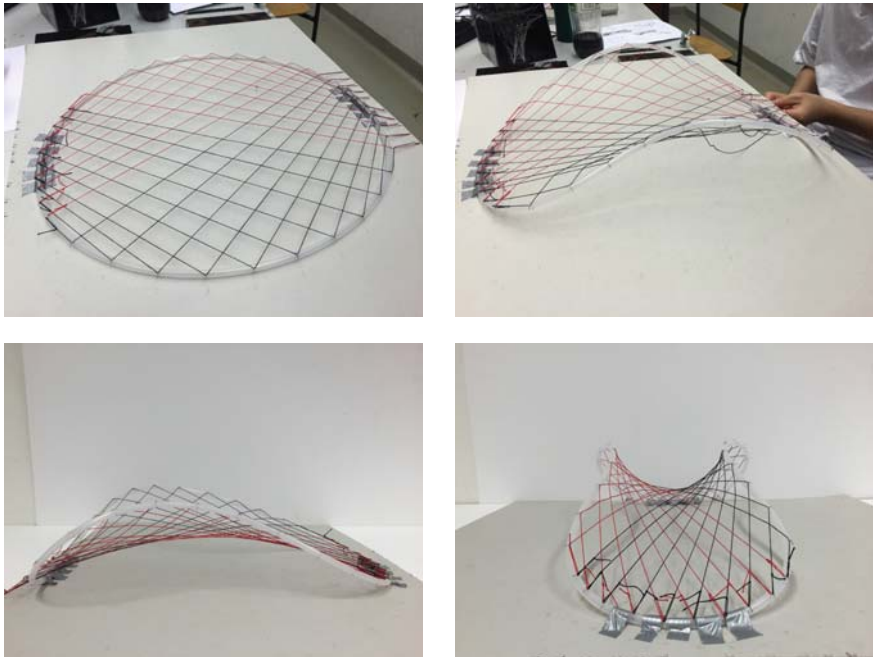

**FIGURE 3_6:** incremental tensioning model. (*Source: Jingcheng Chen, Olga Kalina)*

## Study of Fabrication Process

According to the definition of bending-active structure from Julian Lienhard, we understand that the frame should be initially planar. Therefore, a fabrication process should be considered to bend the frame.

In the very beginning we thought the frame can be bent by gradually adding cables and tension them -- we call incremental tensioning.(Figure 3_6) As you can see the frame was planar in the first place, and by adding cable through a certain order, the frame will be bent gradually into shape.

The model had several continuous cables going through the anchor points to the tensioning device on one side of the rod through which all the cables has been tensioned.

The process was quite impressive, but the result has declined from the certain picture that we wanted to have. The problem was that with this methodology we can not to have more that two sides shape due to the complexity. Also the shape was different than the simulation we had before. In addition to the physical test we practised on the computational simulations.

However, such idea leads us to our next step where we decided to combine two our attempts to make our structure, using tensioning cables instead of the membrane.

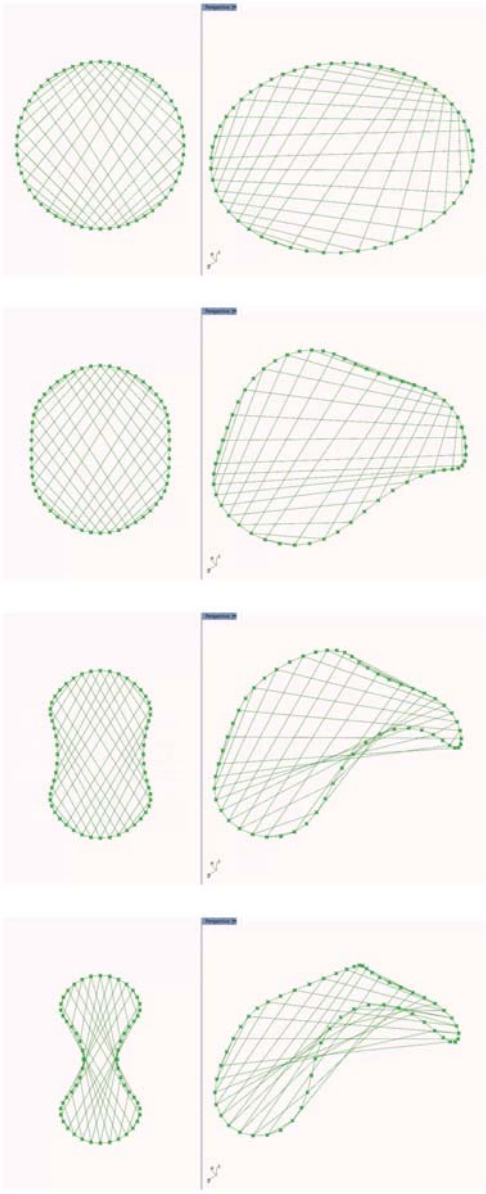

**FIGURE 3_7:** simulation of incremental tensioning model. (*Source: Jingcheng Chen, Olga Kalina)*

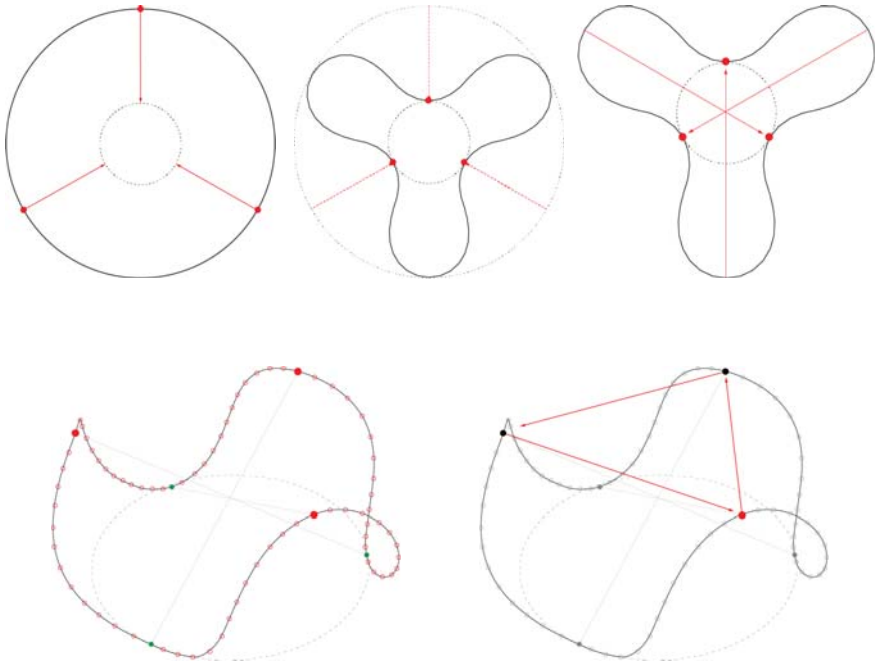

**FIGURE 3_8:** process of bending the frame. (*Source: Jingcheng Chen, Olga Kalina)*

## Study of Fabrication Process

After the decision of the certain form and using a cable to tension, we started to study the weaving syntax specially for cables.

We designed a general rule for the cables to stabilize the whole structure(Figure 3_8). The very first step is to create a closed circle with three anchor points. Second, we bring and connect opposite points close to the middle on a board. Then the other three points on peaks of the sides have to be moved and fixed at upright position with some additional cable connections going in the opposite direction to the floor.

After the frame divided equally and properly fixed, we went further by applying additional cables from side to side through a specific movement syntax(which described on the next page).

Before finding the right order of placing the cables, we made a lot physical model experiments(Figure 3_9).

First attempts were not successful as the cables were not placed equally from each of the side, which causes asymmetrical form. The other problem was that we couldn't find a solution to distribute evenly at all the space between the sides. After some tests we figured a certain weaving syntax that will be shown on next page.

**FIGURE 3_9:** physical model experiments on weaving syntax. (*Source: Jingcheng Chen, Olga Kalina)*

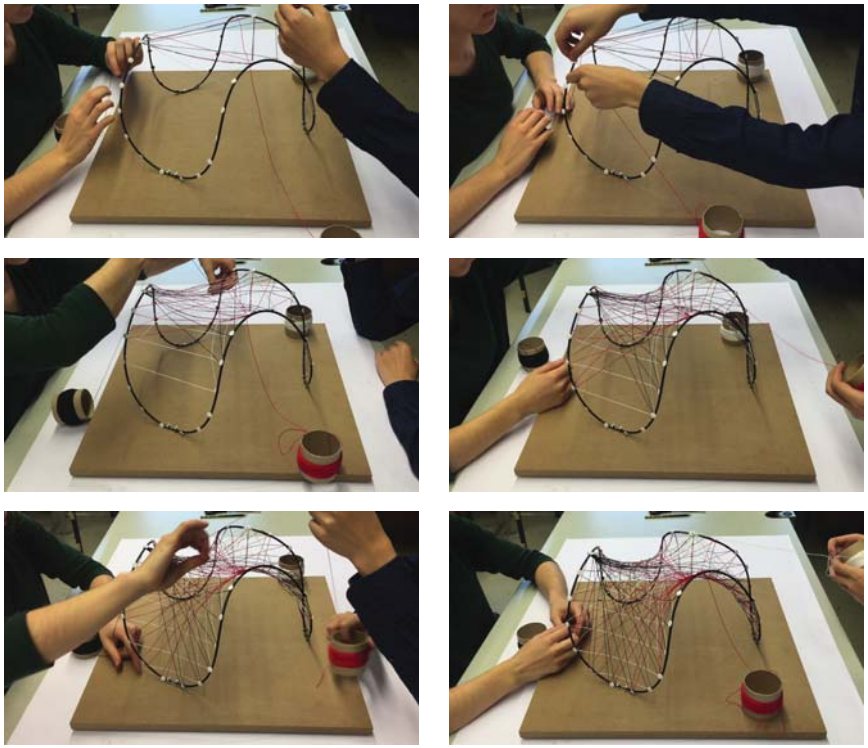

**FIGURE 3_10:** building process of physical model. (*Source: Jingcheng Chen, Olga Kalina)*

## Cable Fabrication Syntax

The table above represents the order of the fabrication of the cables. The process can be described as following :

There are three top points with three separate spools of cables (we choose three different colours for better visual understanding). Each colour has to be placed in a triangle through the top points one by one, coming back to the first point. Then continue doing triangles through the next points located lower previous.

The cables of each colour have to be placed alternatively each other from one side to another until coming to the opposite two top points.

The table on the right presents the steps of placement the cables by colouring them.

The most intrigue part of placing the cables is that the force should be evenly and finely applied while fixing them at anchor points for avoiding a sagging of the previously placed cables.

At the end when all cables are in place, first three temporary forced lines have to be cut. Then all cables became tensioned

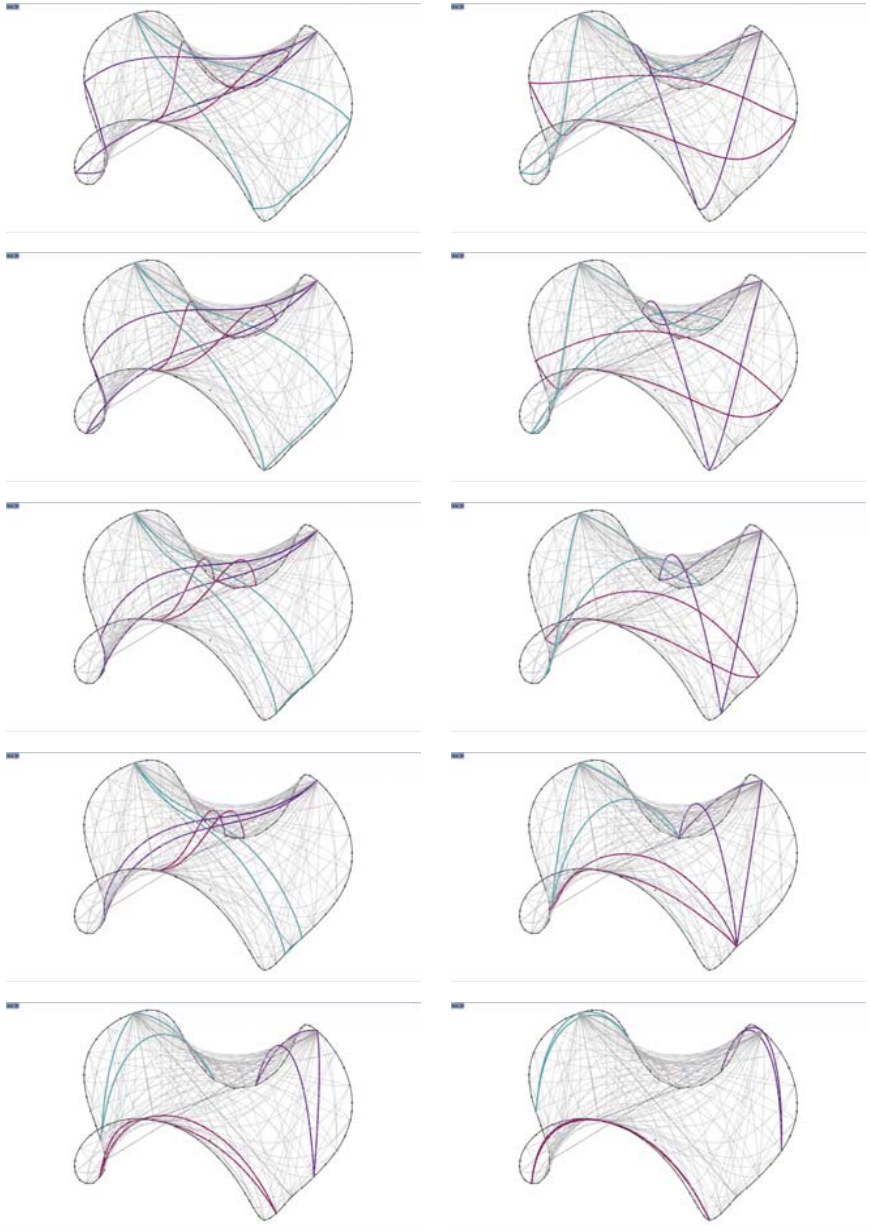

**FIGURE 3_11:** building process of physical model. (*Source: Jingcheng Chen, Olga Kalina)*

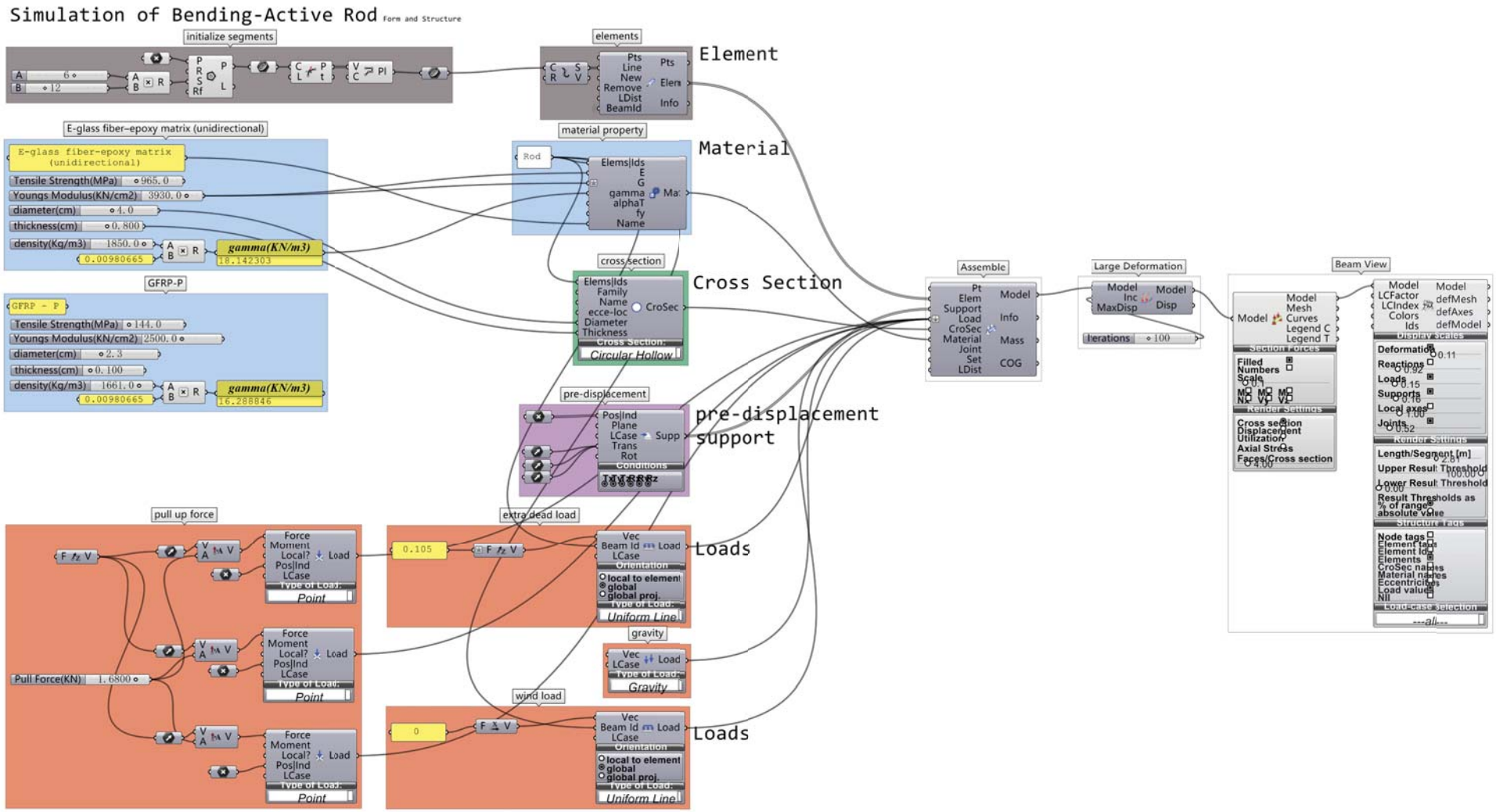


**FIGURE 4_1:** karamba working canvas. (*Source: Jingcheng Chen, Olga Kalina)*

$$\frac{1}{r} = \frac{M}{E \cdot I} \quad (1) \qquad \sigma = \frac{E \cdot I}{r \cdot w} = \frac{E \cdot t}{2 \cdot r} \quad (2)$$

*Table 1: Material dependent elastic bending radii*

| Material | Youngs Modulus E [N/mm ] | tensile strength 60% fyc [N/mm ] | minimal radius as a factor of thickness |
|---|---|---|---|
| CFRP-HAT | 165000 | 1680 | 49*t |
| GFRP-P | 25000 | 144 | 87*t |
| Plywood | 11000 | 30 | 183*t |
| Aluminium | 70000 | 120 | 292*t |
| Steel | 210000 | 213 | 493*t |

**FIGURE 4_2:** material properties. (*Source: ICD, form and structure(2015))*

$$\sigma = \frac{E \cdot I}{r \cdot w} = \frac{E \cdot t}{2 \cdot r}$$

$$E = 25 \ GPa$$
$$\sigma = 144 \ MPa$$
$$r = 2 \ m$$

$$t = \frac{2 \cdot r \cdot \sigma}{E} = \frac{2 \cdot 2m \cdot 144N/mm^2}{25000N/mm^2} = 0.023m$$

**FIGURE 4_3:** GFRP configurations and calculations. (*Source: Jingcheng Chen, Olga Kalina)*

Dead Load:

SelfWeight + Cable + Connector

Cable:

$$D = 0.001 \ m$$
$$\rho = 6.982 \ Kg/Km$$
$$L = 859 \ m$$
$$m = L \cdot \rho = \ 859m \cdot 6.982 \ Kg/Km = 5.99\text{Kg}$$

$$G = m \cdot g = \ 5.99 \ Kg \cdot 9.8N/Kg = 0.059KN$$

Connector:

$$V = 1.36 \times 10^{-5} \ m^3$$
$$N = 44$$
$$m = V \cdot \rho = \ 1.36 \cdot 10^{-5} \ m^3 \cdot 44 \cdot 7870 \ Kg/m^3 = 4.71Kg$$

$$G = m \cdot g = \ 4.71 \ Kg \cdot 9.8N/Kg = 0.046KN$$

**FIGURE 4_4:** calculations of self weight from joints and cables. (*Source: Jingcheng Chen, Olga Kalina)*

## Material and Load Calculations

We developed the simulation process in Karamba as shown in the last page(Figure 4_1). As required by Karamba, we have to define structural elements, materials, forces, supports that would be constructed in reality.

In attempt to simulate the whole system, after our form finding process, we need to define a proper material for the structure. Firstly we looked for the bending-active material glass fiber reinforced polymer(GFRP)(Figure 4_2). GFRP usually has the Young's Modules of 25 Gpa, and bending strength of 144 Mpa. It is generally the most common material for a bending-active rod. According to the formula, we can deduce that the maximum thickness of the rod that can bend into our frame shape is around 2.3 cm.

Whereas considering the forces of the system, it is essential to also include the self-weight of all the joints and connections. So we calculated that we have around 859 m of steel cable in total, with the diameter of 1 mm. Also, we have 44 joints, which weighs 0.05 kg for each. These two in total counts for approximately 10 kg.

The simulation process can be divided into 4 steps. Firstly we add predefined forces to squeeze the circular frame into triangular form. Secondly, three outside points are pulled up into positions. Thirdly self-weights are added onto the structure. Fourthly an after tension is implemented to resist the deformation caused by self-weight.

As you can see from the diagram that, in the first simulation process, the GFRP material can not bear the self-weight and totally collapsed, which proves that it is not practical to use GFRP material. A better material is needed for the demand form of structure.

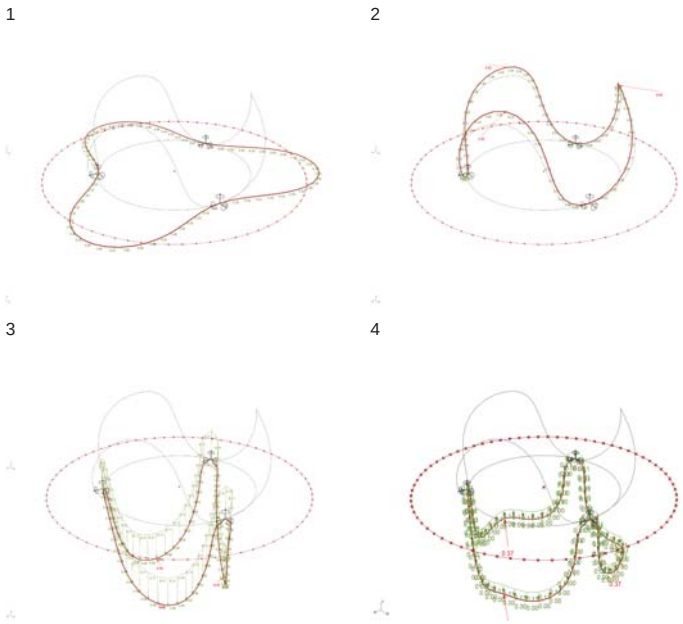


**FIGURE 4_5:** simulation visualization. (*Source: Jingcheng Chen, Olga Kalina)*

1. pre-displacement force
2. initial tension force
3. dead load of self weight
4. retensioning of the system to resist welf-weight

**TABLE 1.1**
**Tensile Properties of Some Metallic and Structural Composite Materials**

| Material[a] | Density, g/cm³ | Modulus, GPa (Msi) | Tensile Strength, MPa (ksi) | Yield Strength, MPa (ksi) | Ratio of Modulus to Weight,[b] $10^6$ m | Ratio of Tensile Strength to Weight,[b] $10^3$ m |
|---|---|---|---|---|---|---|
| SAE 1010 steel (cold-worked) | 7.87 | 207 (30) | 365 (53) | 303 (44) | 2.68 | 4.72 |
| AISI 4340 steel (quenched and tempered) | 7.87 | 207 (30) | 1722 (250) | 1515 (220) | 2.68 | 22.3 |
| 6061-T6 aluminum alloy | 2.70 | 68.9 (10) | 310 (45) | 275 (40) | 2.60 | 11.7 |
| 7178-T6 aluminum alloy | 2.70 | 68.9 (10) | 606 (88) | 537 (78) | 2.60 | 22.9 |
| Ti-6A1-4V titanium alloy (aged) | 4.43 | 110 (16) | 1171 (170) | 1068 (155) | 2.53 | 26.9 |
| 17-7 PH stainless steel (aged) | 7.87 | 196 (28.5) | 1619 (235) | 1515 (220) | 2.54 | 21.0 |
| INCO 718 nickel alloy (aged) | 8.2 | 207 (30) | 1399 (203) | 1247 (181) | 2.57 | 17.4 |
| High-strength carbon fiber–epoxy matrix (unidirectional)[a] | 1.55 | 137.8 (20) | 1550 (225) | — | 9.06 | 101.9 |
| High-modulus carbon fiber–epoxy matrix (unidirectional) | 1.63 | 215 (31.2) | 1240 (180) | — | 13.44 | 77.5 |
| E-glass fiber–epoxy matrix (unidirectional) | 1.85 | 39.3 (5.7) | 965 (140) | — | 2.16 | 53.2 |
| Kevlar 49 fiber–epoxy matrix (unidirectional) | 1.38 | 75.8 (11) | 1378 (200) | — | 5.60 | 101.8 |
| Boron fiber-6061 A1 alloy matrix (annealed) | 2.35 | 220 (32) | 1109 (161) | — | 9.54 | 48.1 |
| Carbon fiber–epoxy matrix (quasi-isotropic) | 1.55 | 45.5 (6.6) | 579 (84) | — | 2.99 | 38 |
| Sheet-molding compound (SMC) composite (isotropic) | 1.87 | 15.8 (2.3) | 164 (23.8) | | 0.86 | 8.9 |

[a] For unidirectional composites, the fibers are unidirectional and the reported modulus and tensile strength values are measured in the direction of fibers, that is, the longitudinal direction of the composite.
[b] The modulus–weight ratio and the strength–weight ratios are obtained by dividing the absolute values with the specific weight of the respective material. Specific weight is defined as weight per unit volume. It is obtained by multiplying density with the acceleration due to gravity.

**FIGURE 4_6:** material properties. (*Source: P.K. Mallick (2007))*

$$E = 39.3\ GPa$$
$$\sigma = 965\ MPa$$
$$r = 2\ m$$

$$t = \frac{2 \cdot r \cdot \sigma}{E} = \frac{2 \cdot 2m \cdot 965N/mm^2}{39300N/mm^2} = 0.098m$$

**FIGURE 4_7:** e glass fiber-epoxy matrix configurations and calculations. (*Source: Jingcheng Chen, Olga Kalina)*

After the first trial of GFRP material, we realized that it is essential to find another material that has stronger Young's Modules and bending strength. At the same time it still needs to be elastic enough as bending-active material. We then looked for another material called E glass fiber-epoxy matrix, which has Young's Modules of 39.3 Gpa and bending strength of 965 Mpa. With this material property, to reach the minimum radius of 2 m required by the form, we can get maximum 9.8 cm diameter of the rod frame.

Following this configuration, we tried rod diameter of 3 cm and 4 cm respectively. As shown in next page(Figure 4_8,Figure 4_9), for the 3 cm rod there still exists a strong buckling when the dead load is added. Whereas 4 cm diameter of the rod can resist the buckling and by re-tensioning we can achieve the desired form, which proves that this material is practical with the rod diameter of 4 cm.

We can also visualize the moments and forces from three directions, which gives an intuitive impression of how the rod bears the forces and moments.(Figure 4_8)

1

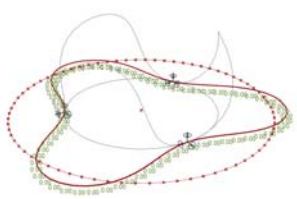

2

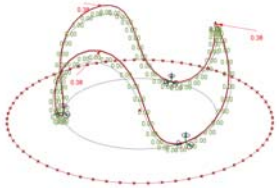

3

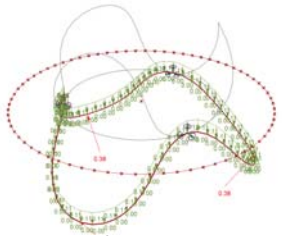

4

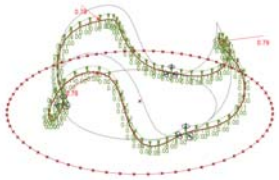

**FIGURE 4_8:** e glass fiber-epoxy matrix with 3 cm diameter. (*Source: Jingcheng Chen, Olga Kalina)*

1

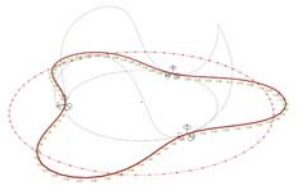

2

3

4

**FIGURE 4_9:** e glass fiber-epoxy matrix with 4 cm diameter. (*Source: Jingcheng Chen, Olga Kalina)*

1

2

3

4

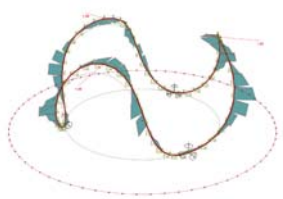

5

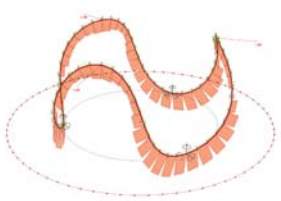

6

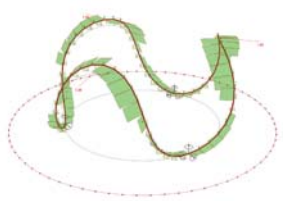

**FIGURE 4_10:** visualization of bending moment and axial forces. (*Source: Jingcheng Chen, Olga Kalina)*

1. X-Axis bending moment
2. Y-Axis bending moment
3. Z-Axis bending moment
4. X-Axis axial force
5. Y-Axis axial force
6. Z-Axis axial force

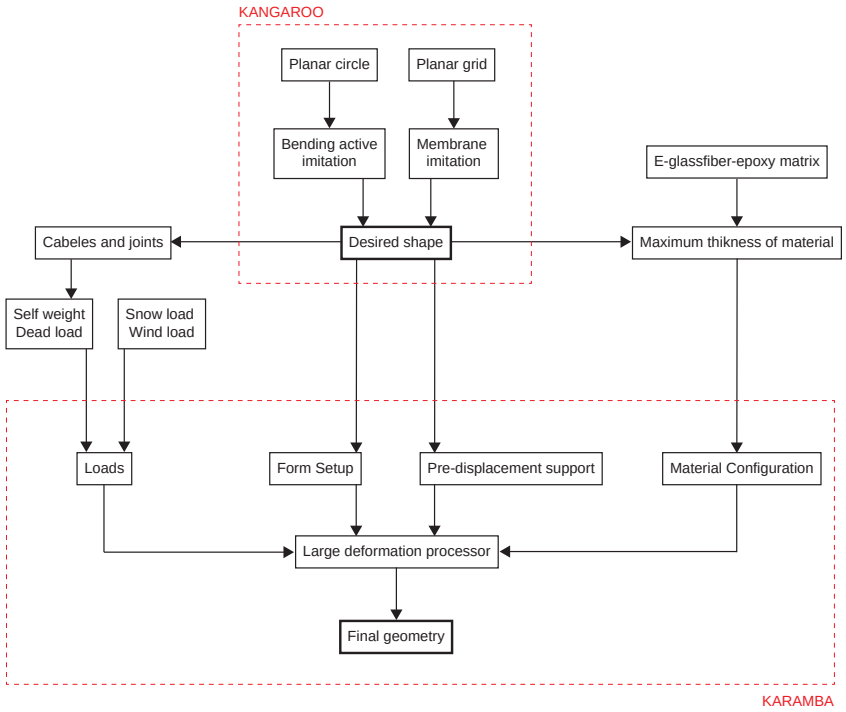


**FIGURE 4_11:** digital roadmap of simulation. (*Source: Jingcheng Chen, Olga Kalina)*

### Digital Roadmap

To conclude, we first used kangaroo to find the desired form, by imitating the performance of membrane and bending-active material. Based on this form we calculated proper material configurations and set up the simulation model in karamba. After choosing special assemble processor will we get the final geometry.

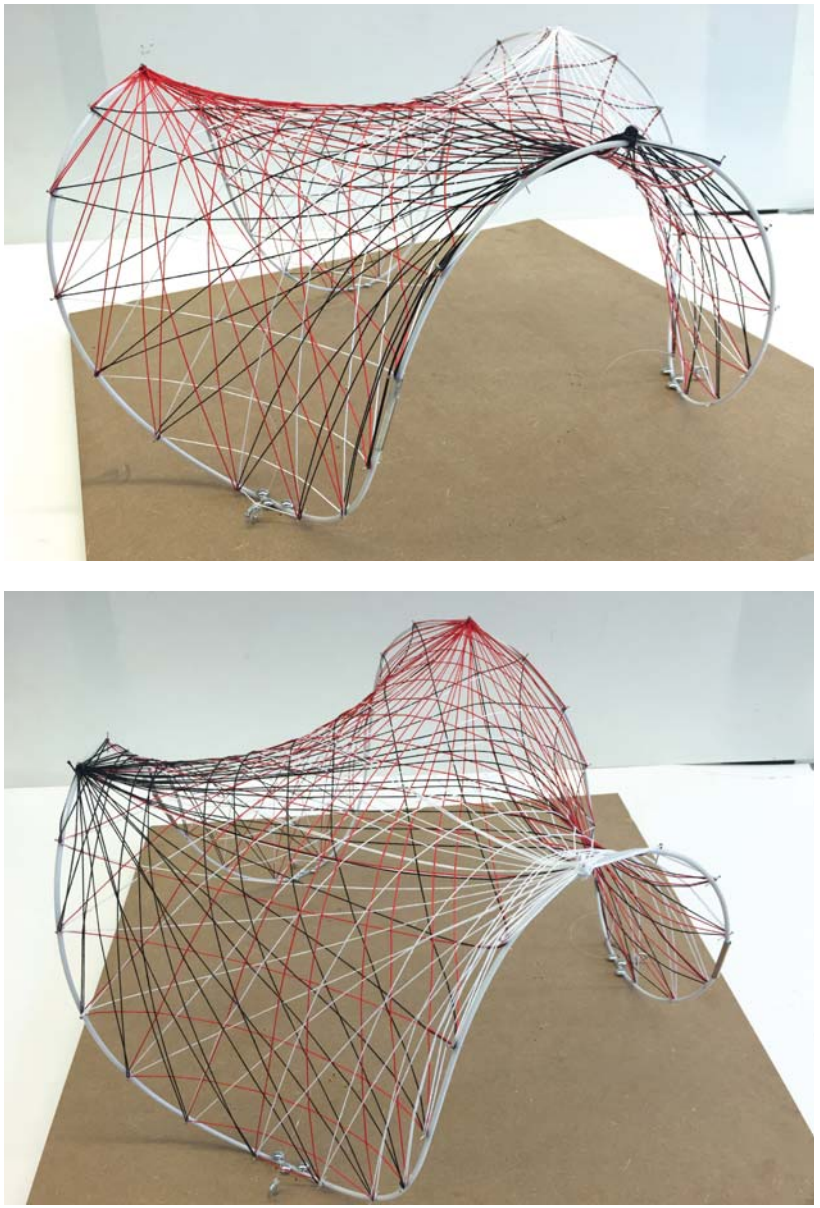

**FIGURE 4_12:** final physical model. (*Source: Jingcheng Chen, Olga Kalina)*

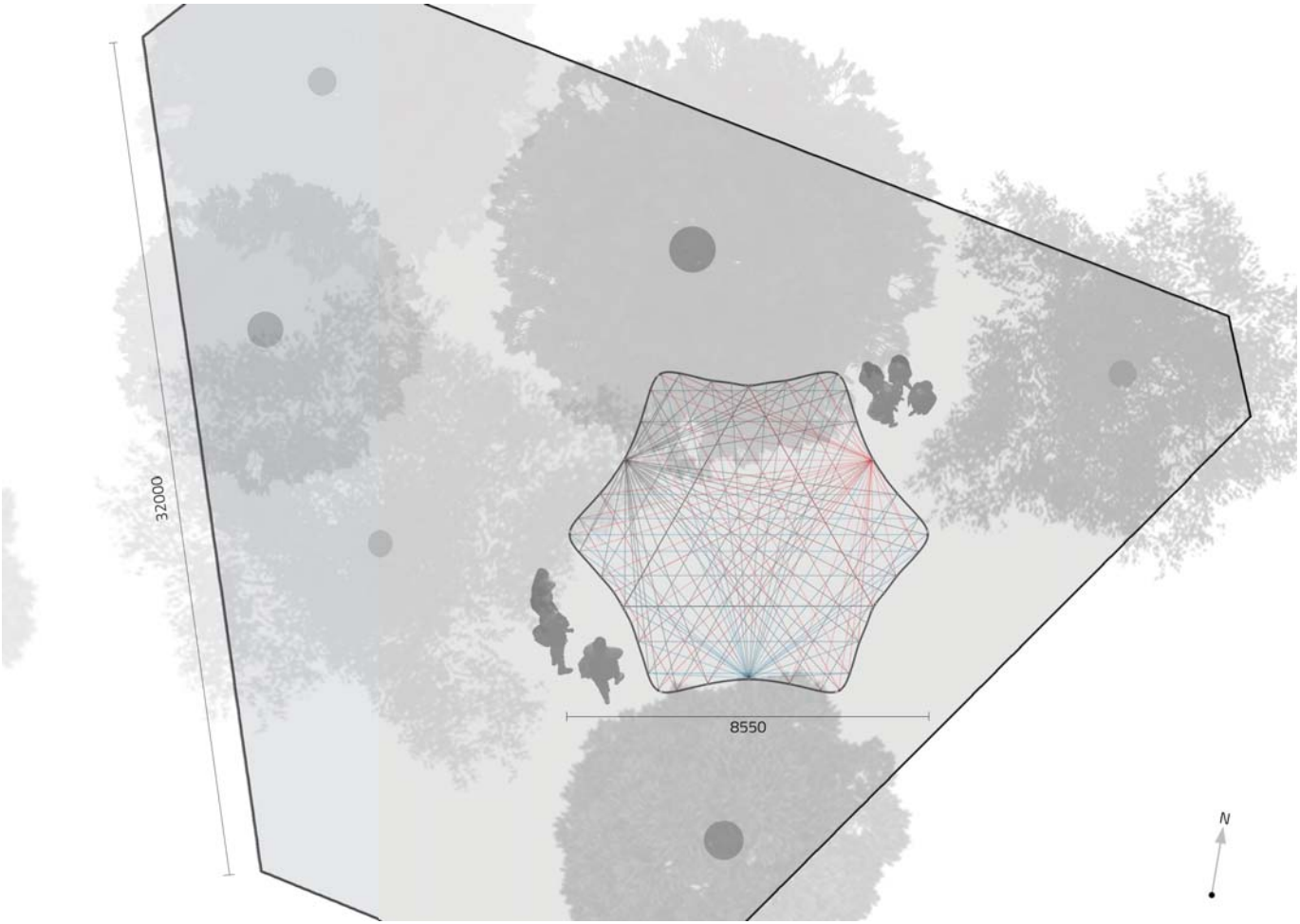


**FIGURE 5_1:** Architectural drawing. Top view. (*Source: Jingcheng Chen, Olga Kalina* )

## Architectural description

From the architectural point of view the structure has some advantages. From the top view you can see that the structure is symmetrical, which allows three entrance through each of them people can cross the space.

Moreover, such structure can be modular. There is a chance to scale the module into small scales and each structural module can stand apart from each other and organize a complex space.

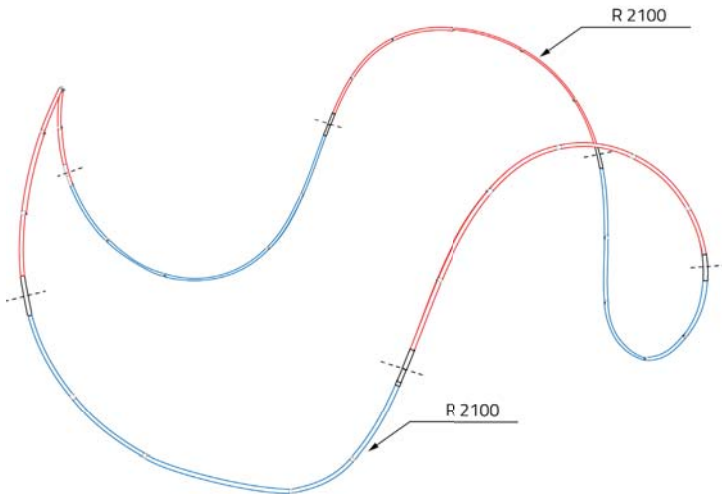


**FIGURE 5_2:** Rod subdivision. (*Source: Jingcheng Chen, Olga Kalina* )

## Rod Subdivision

According to the length limitation of material and transportation, we were restricted to the division of cutting the rod. The structure has initially around 37 m in length in total(Figure 5_2). In this case, we cut the rod into six pieces with each piece of around 6.2 m. At the same time we guaranteed that all the connection position has the smallest curvature(biggest radius) while all the divided rods have the same shape.

Rod-rod connection is designed short and simple(Figure 5_6), in order not to affect the performance of bending-active rod and keep as light as possible as well.

Besides, we have altogether 44 cable-rod joints(Figure 5_5), each one is designed as light and small as possible. In the construction process they should be embedded in the rod before actually start bending the rod.

An anchor joint to fix the structure on the ground is also designed. Since our structure bears rare wind load, it is possible for us to have a small anchor joint without affecting the site too much.

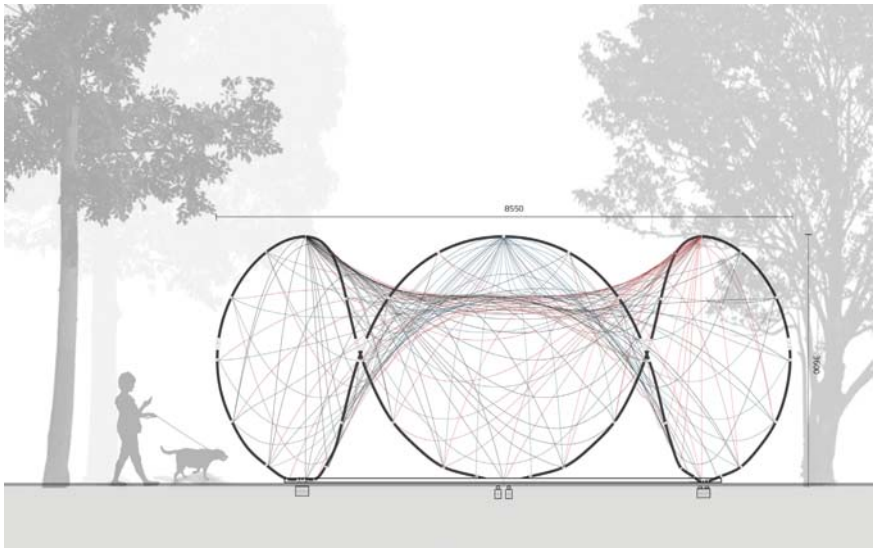


**FIGURE 5_3:** Architectural drawing. South elevation. (*Source: Jingcheng Chen, Olga Kalina* )

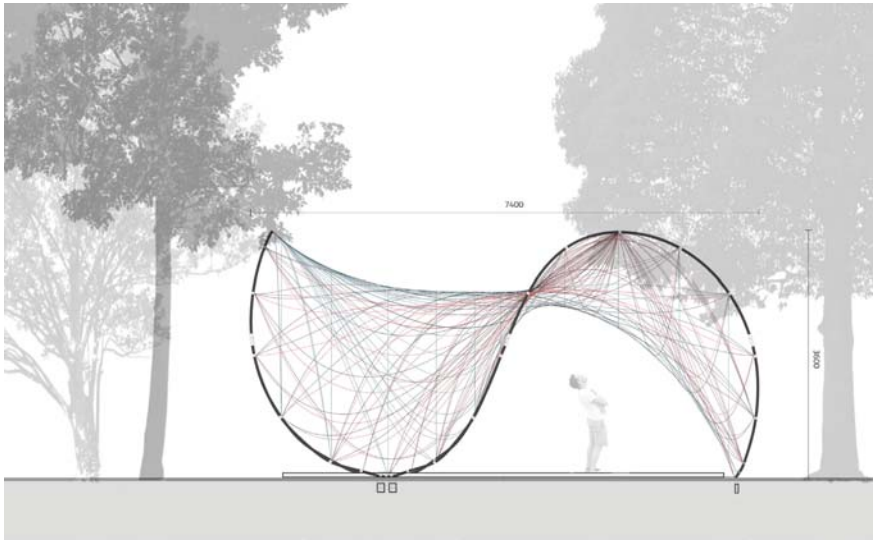


**FIGURE 5_4:** Architectural drawing. East elevation. (*Source: Jingcheng Chen, Olga Kalina* )

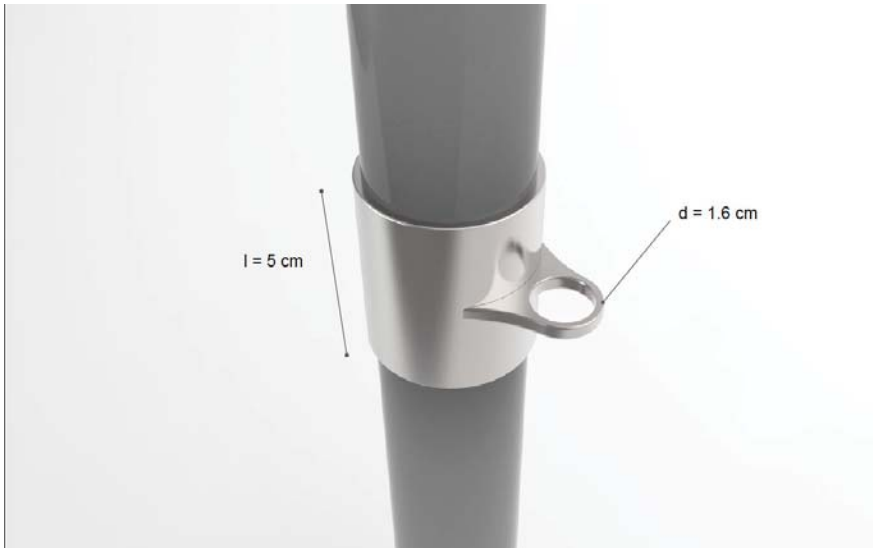


**FIGURE 5_5:** Architectural drawing.Anchor. (*Source: Jingcheng Chen, Olga Kalina* )

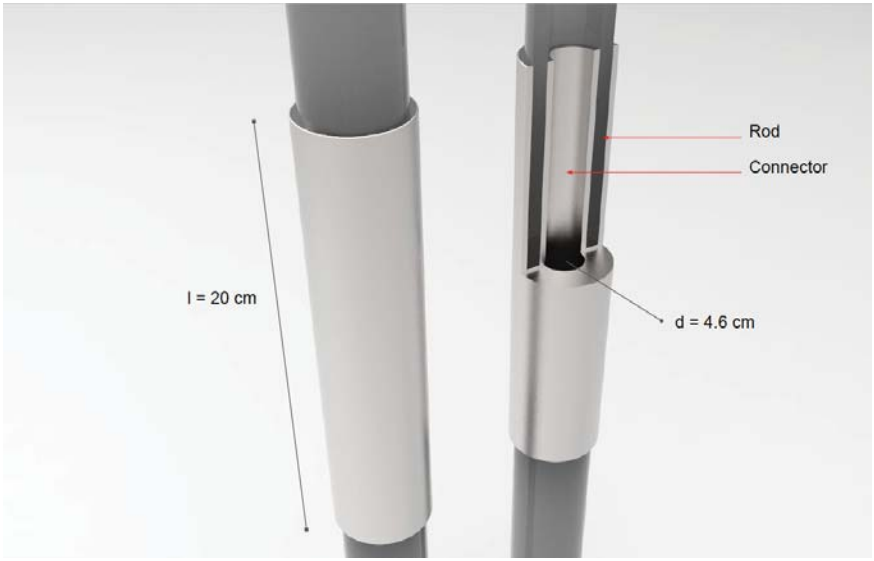


**FIGURE 5_6:** Architectural drawing.Rod-Rod connection . (*Source: Jingcheng Chen, Olga Kalina* )

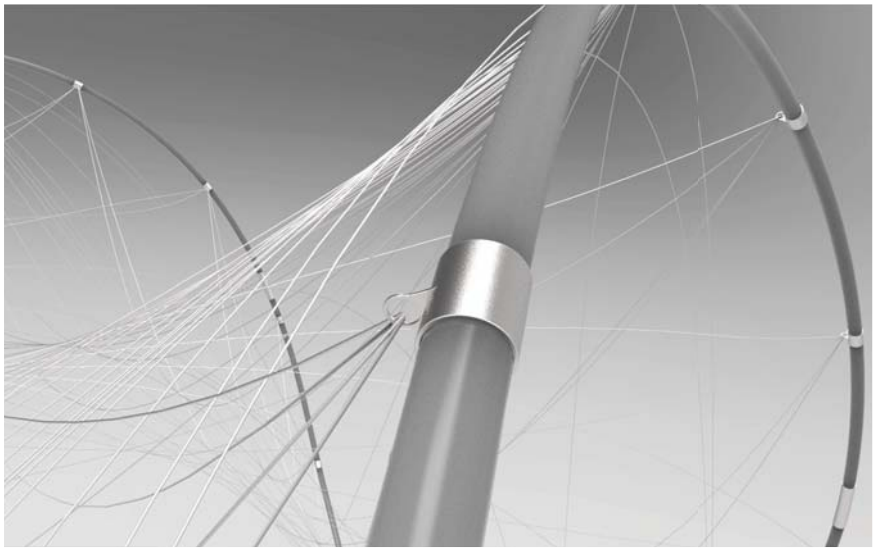

**FIGURE 5_7:** Architectural drawing.Anchor. (*Source: Jingcheng Chen, Olga Kalina* )

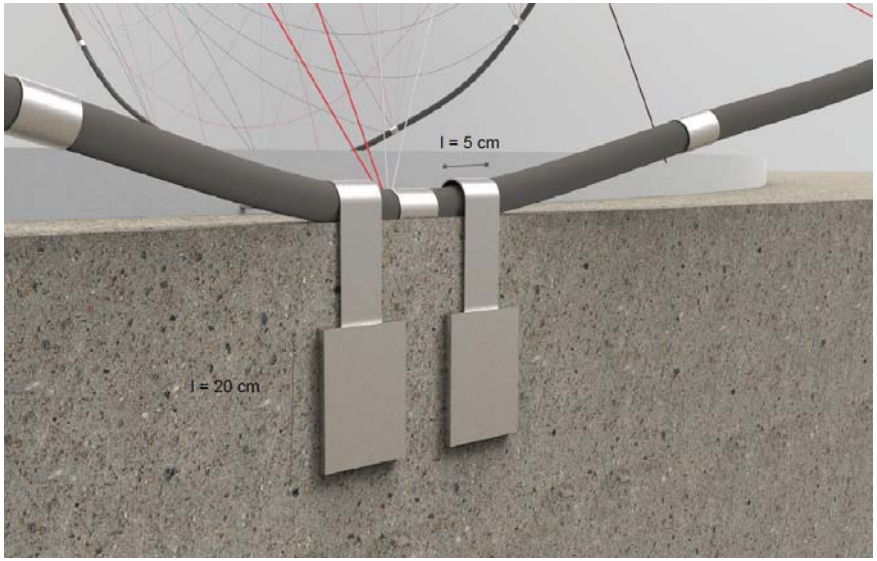


**FIGURE 5_8:** Architectural drawing.Floor fixation. (*Source: Jingcheng Chen, Olga Kalina* )

## References


1. **Julian Lienhard (2014)**, Bending-Active Structures, form-finding strategies using elastic deformation in static and kinematic systems and the structural potentials therein

2. **M. C. Phocas, O. Kontovourkis & K. Alexandrou (2014)**, The structural design and construction of a cable bending-active structure

3. **P.K. Mallick (2007)**, Fiber Reinforced Composites Materials, Manufacturing and Design

4. **Alvin Huang (2014)**, Pure Tension Pavilion, An experiment in dynamic mesh relaxation

5. **Julian Lienhard ·Jan Knippers (2013)**, Considerations on the Scaling of Bending-Active Structures

6. **Paul Nicholas and Martin Tamke (2013)**, Computational Strategies for the Architectural Design of Bending Active Structures

7. **Lienhard, J, Alpermann, H, Gengnagel, C, & Knippers, J (2012)**, Active Bending, a Review on structures where bending is used as a self-formation process

8. **Sean Ahlquist · Ali Askarinejad · Rizkallah Chaaraoui · Ammar Kalo · Xiang Liu · Kavan Shah (2014)**, Postforming Composite Morphologies: Materialization and design methods for inducing form through textile material behavior

9. **Sean Ahlquist · Achim Menges (2013)**, Frameworks for Computational Design of Textile Micro-Architectures and Material Behavior in Forming Complex Force-Active Structures